doi: 10.56761/EFRE2024.S3-O-036701

Effect of the presence of a resonator and processes in the cathode-anode gap on the generation mechanism in the axial vircator

E.A. Gurnevich[1,], P.V. Molchanov[2]*

[1]*Technology Innovation Institute, Abu Dhabi, UAE*
[2]*Institute for Nuclear Problems, Belarusian State University, Minsk, Belarus*
[*]*evgeny.gurnevich@tii.ae*

Abstract. The analysis of the generation phenomena in the axial vircator has been conducted for two scenarios: with and without considering cathode-anode gap processes. A comparative analysis between the two principal layouts: injection of the high-current electron beam into a simple drift tube and into the resonator, is also presented. It is observed that the generation mechanisms in vircators under the two scenarios are significantly different from each other, and the generation frequencies differ radically as well. When considering the cathode-anode gap phenomena, the oscillations of electrons between the real and virtual cathodes, as well as the oscillations of the VC itself, occur synchronously and always with the same frequency. The dependencies of generation efficiency on the beam current, cathode-anode gap value, and anode mesh transparency were calculated. It is observed that for each geometry of the resonator, there is an optimal value of anode mesh transparency, maximizing the generation efficiency and power. The presented findings encourage further research on the physics of electron beams with virtual cathodes.
Keywords: axial vircator, virtual cathode, electron beams, high power microwaves.

1. Introduction

Virtual cathode oscillators (vircators) are oscillators capable of generating sub-gigawatt peak power microwaves. The relativistic version of the vircator has been the research focus for many years in the high-power microwave HPM community. Despite the numerous studies reported in the literature, the generation mechanism in vircators remains a topic of ongoing discussion. Some studies [1–2] associate the generation frequency with the plasma frequency of the electron beam, while others associate it with the oscillation frequency of electrons in the "cathode-virtual cathode (VC)" potential well [3]; there are studies that claim that these two frequencies always coincide [4]. Furthermore, the impact of anode mesh transparency on generation power has not yet been thoroughly analyzed and defined.

The most common theoretical model of radiation generation in a vircator can be obtained when neglecting the phenomena occurring in the cathode-anode gap. In this case, a beam with given parameters is injected into the drift tube; the injection plane usually corresponds to the position of the anode mesh in a real system (see Fig. 1). For the one-dimensional case, the theory of such a vircator is described in detail in [1]. One of its most important results is the obtained dependency of the vircator generation frequency on the plasma frequency of the electron beam in the injection plane.

Let the injected beam current be equal to I_{in}. If it exceeds the limiting current for a given system I_{lim}, then the part of the current I_{re} will be reflected to the injection plane, while the other part I_{tr} will pass behind the VC. Then, by the analysis [1], the generation frequency ω is proportional to the beam plasma frequency ω_p:

$$\omega \approx 2.8\omega_{p'}, \tag{1}$$

where

$$\omega_p = \left(\frac{n_0 e^2}{\varepsilon_0 m \gamma_0}\right)^{1/2}, \tag{2}$$

m, e are electron mass and charge, respectively, γ_0 is the electron Lorentz factor in the injection plane, ε_0 is the vacuum permittivity constant, and n_0 is the electron's density in the injection plane, corresponding to the current $I=|I_{in}| + |I_{re}|$.

It is essential, and this is also noted in [1], that the equation (1) is valid only for the one-dimensional case. In addition, this equation in [1] was derived without considering the processes occurring in the cathode-anode gap. Other researchers, taking into account the process of oscillations of beam electrons between real and virtual cathodes, obtained different formulas for the generation frequency [2, 5], in particular $\omega \approx 2.5\omega_{p0}$, where ω_{p0} corresponds to the diode current without taking into account the reflected part of the beam.

In the presented paper, in order to see what results from taking into account the non-one-dimensionality of the beam motion, we will show the results of the simulation of the simplest axial vircator (without cathode-anode gap: just the injection of the beam into the drift tube) in the 2.5D particle-in-cell code XOOPIC [6]. Then, we will include the cathode-anode gap in our simulation. Finally, we will show how the addition of resonating elements into the drift tube affects generation.

2. The geometry of the problem

Three different layouts were considered (Fig. 1). For brevity, we will henceforth refer to them as configuration *1*, *2*, and *3*. In configuration *1*, a cylindrical electron beam with a diameter of 70 mm was injected into a drift tube with a diameter of 100 mm. The beam energy was 525 keV, and the beam current could be set arbitrarily (it was varied from 10 to 21 kA). The initial energy spread in the beam was assumed to be zero. There was no guiding magnetic field in the drift tube. Electrons reflected from the VC and incident back onto the injection plane were excluded from the simulation. The length of the drift tube was 262 mm. The dimensions of the drift tube were chosen for the convenience of comparing the results: they are naturally obtained if all the resonant elements are removed from the three-cavity axial vircator, which we considered earlier in [7] (variant #1).

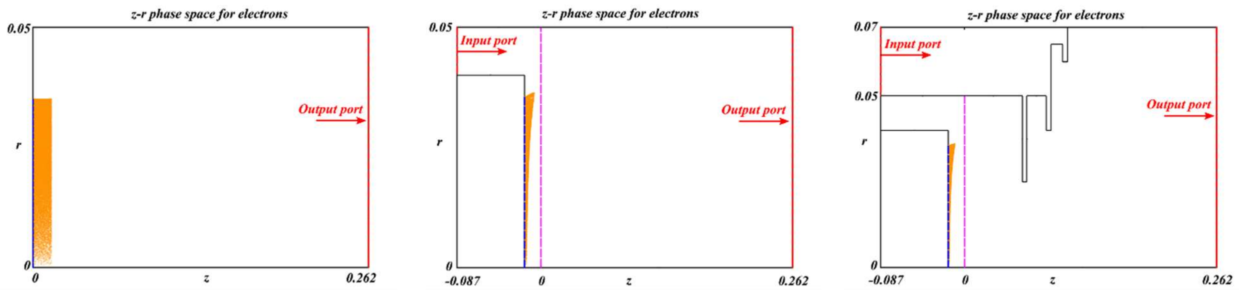

Fig. 1. Simulation domain in XOOPIC. From left to right: configuration *1* – beam injection into the drift tube, configuration *2* – simulation taking into account the cathode-anode gap phenomena, configuration *3* – resonant vircator. The orange color shows the positions of the particles immediately after the start of the simulation; the purple dashed line is the anode mesh. Perfectly conducting boundaries and the axis of symmetry $r = 0$ are indicated in black.

In configuration *2*, instead of injection plane, there was transparent to electrons (100% transparency) perfectly conducting plane, imitating the anode mesh or foil in real vircators. The beam, in this case, was emitted from the cathode (cylinder of 80 mm diameter, at the end of which an emission region with a diameter of 71 mm was specified). The explosive electron emission model was used. To start emission, a TEM wave was injected into the *Input port* of the structure; the amplitude of the wave was chosen to provide the voltage of 525 kV between the cathode and anode in the presence of a beam. With this approach, the beam current was no longer set arbitrarily; the cathode-anode gap value determined it. Therefore, for the convenience of comparing the results for configurations *1* and *2*, the current-voltage characteristics of the diode were calculated in advance.

The configuration *3* was supplemented by introducing resonant elements (diaphragms) into the drift tube. The sizes and positions of the diaphragms were chosen to be the same as in the three-cavity vircators discussed in [7] (the main one is variant #1). Additionaly, it was possible to change the anode mesh's transparency (for electrons).

The radiation power for all configurations was determined by integrating the Poynting vector over the drift tube section near the O*utput port*. The radiation spectra were analyzed using the Fourier transform of the electric field measured near the *Output port*. In addition, in the simulation we measured the total current passing through the drift tube at different distances z_i from the injection plane (or anode mesh): $z_i = 2i$ mm for i=0–15, and also at z_{16} = 40 mm and z_{17} = 50 mm.

3. The simulation results

Fig. 2 shows the calculated radiation power and efficiency dependencies on the electron beam current. It can be seen that for the first two problems, the radiation power quickly reaches saturation with increasing beam current and then changes only slightly, remaining at the level of 90–100 MW for problem *1* and 100–120 MW for problem *2*, even for beam powers above 10 GW. The radiation efficiency has a weakly expressed maximum (~1.5%) at a certain optimal beam current value. As the beam current increases above this value, the efficiency decreases monotonically. For the system under consideration, the maximum efficiency corresponds to a current I_{in} of 12 kA, approximately 2.6 times greater than the limiting current I_{lim} for a given geometry. For configuration *3* (resonant vircator), radiation power and efficiency behave completely differently from those for configurations *1* and *2*; it is discussed below.

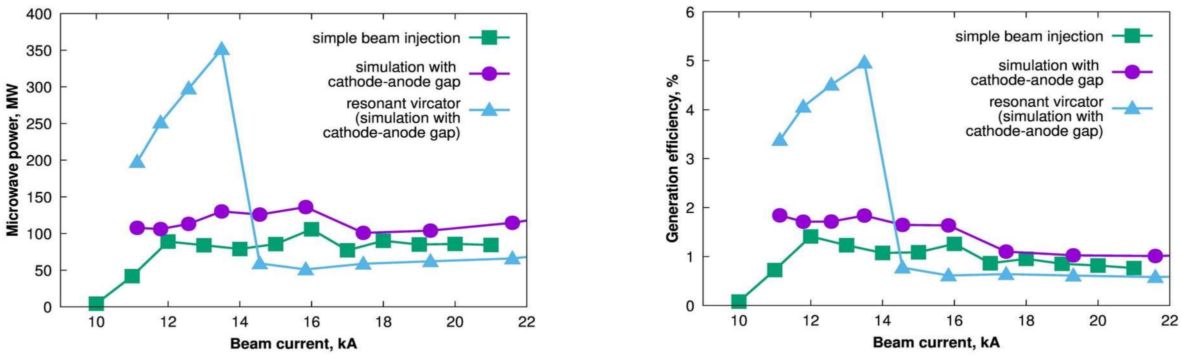

Fig. 2. Power (left) and efficiency (right) of generation in an axial vircator at different beam currents.

Fig. 3 (left) shows the calculated dependence of the generation frequency on the value of the injected current for problem *1*. For clarity, in the same figure, the curve $\omega \approx 2.8\ \omega_p$ is shown, where the calculation of the plasma frequency was carried out for a beam with 70 mm diameter, the energy of 525 keV, and the current $I = |I_{in}| + |I_{re}|$ in full accordance with [1] (I_{re} was calculated using the data of current monitors). As expected, the frequency increases with increasing beam current. However, it can be seen that predictions of the one-dimensional theory (1)–(2) don't agree well with the results of calculations, which, in principle, was expected: the beam in the system under consideration near the VC demonstrates very complex dynamics, and the actual density of the electron cloud can differ significantly from that which would be for a one-dimensional beam.

Significant changes occurred, however, in the radiation spectrum for configuration *2*: the main generation frequencies became significantly lower (compared to those of configuration *1*) at the same beam currents (see Fig. 3, right). At the same time, a detailed spectral analysis of the field and current signals does not show any additional peaks at frequencies observed for configuration *1*. The generation frequencies turn out to be approximately inversely proportional to the cathode-anode gap, which is visible in Fig. 4. They are also quite satisfactorily described (being only ~7% higher) by the well-known formula [3, 8]:

$$f\left[\text{GHz}\right] \approx \frac{4.77}{d\left[\text{cm}\right]} \log\left(\gamma_0 + \sqrt{\gamma_0^2 - 1}\right). \tag{3}$$

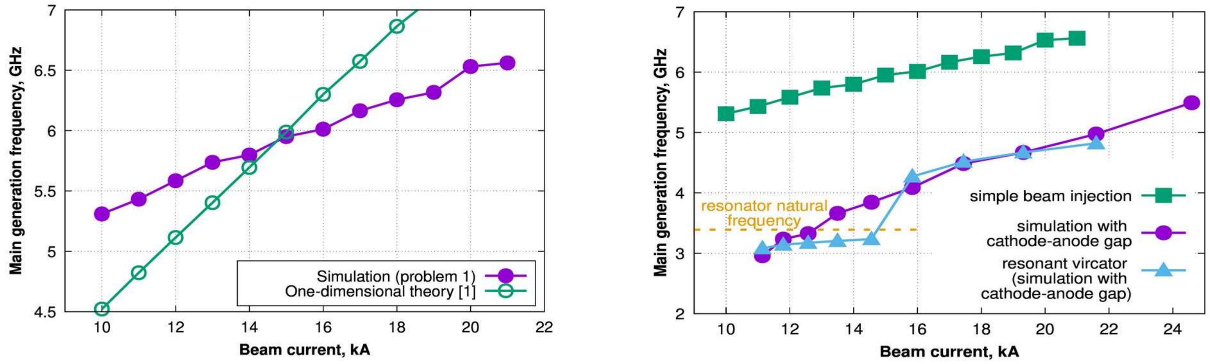

Fig. 3. Generation frequency in a vircator. Left: comparison of the simulation results for configuration *1* with the predictions of one-dimensional theory [1], right: main generation frequencies for all considered configurations.

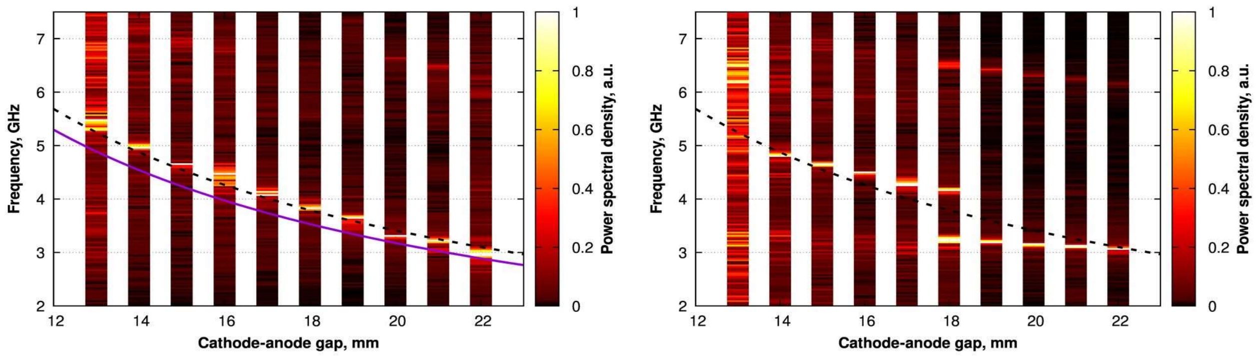

Fig. 4. Radiation spectra of vircator at various cathode-anode gaps: left: configuration *2*, right: configuration *3*. The solid line shows the prediction of the formula (3), and the dashed line is the approximation of the form $f = const/d$.

For configuration *3*, in a certain range of beam current values (10–14 kA in the example shown in Fig. 3), the main radiation frequency is almost independent of the current value (or cathode-anode gap). In this range, highly efficient generation is observed (see Fig. 2), and the radiation power reaches 350 MW. With a further increase in the beam current, the generation frequency increases abruptly. It begins to behave in the same way as in the case of a non-resonant vircator (problem *2*), changing inversely proportional to the gap value *d*. Note that the radiation frequency in the high-efficiency mode turns out to be close to the resonator's natural frequency. For all variants of three-cavity resonant vircators, we got the same result: the oscillation frequency of the VC is locked to the natural (unperturbed) frequency of the resonator ω_{res}, unless the initial absolute value of the detuning $\delta\omega_{res} = \omega_{vc,0} - \omega_{res}$ was not too high ($\omega_{vc,0}$ here is the generation frequency in non-resonant vircator (configuration *2*)). Note also that when the generation frequency is locked to the resonator frequency, higher harmonics are observed in the radiation spectrum (see Fig. 4).

Let us recall that, according to the basic theory [1], the total beam current in a vircator can be expressed as the sum of constant and oscillating components. To get the oscillating component, we conducted a Fourier analysis of the data from all current monitors. Fig. 5 shows the dependencies of the amplitude of the oscillating current (1st harmonic) on the longitudinal coordinate z for different beam currents. From Fig. 5 one can see that the amplitude of the oscillating current has a maximum in the region where the VC is located. Naturally, the position of this maximum shifts to the lower z values as the beam current increases. For problem *1*, a plateau is observed near $z = 0$ (the modulated beam returns to the injection plane, maintaining the degree of its modulation approximately constant).

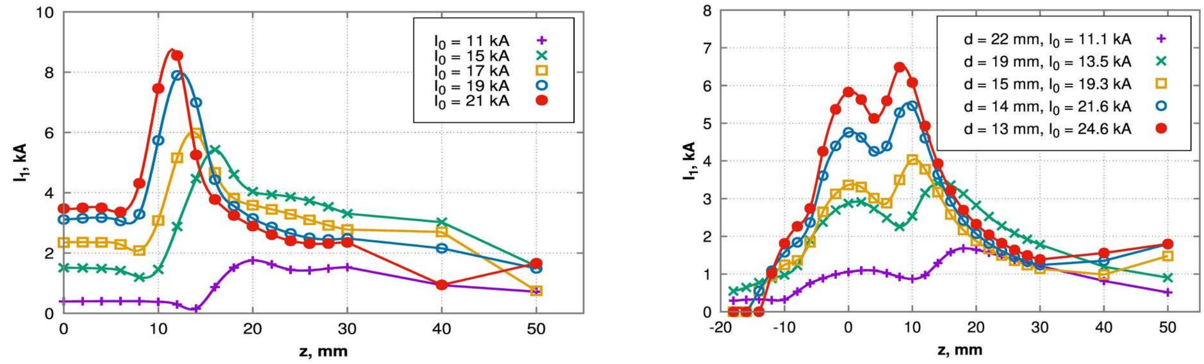

Fig. 5. Amplitudes of the oscillating current component versus the longitudinal coordinate for different beam currents (cathode-anode gaps): simulation results for configuration *1* (left) and configuration *2* (right).

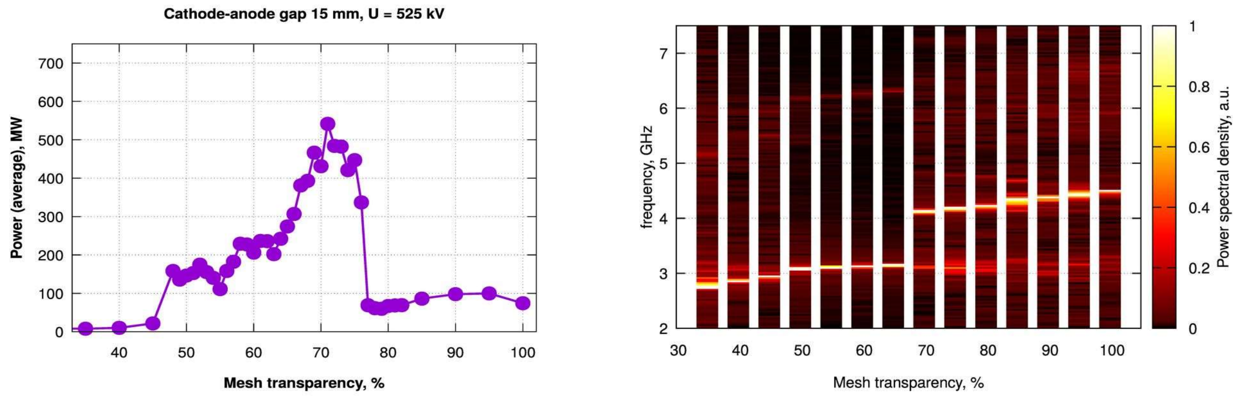

Fig. 6. The example of obtained dependence of radiation power on the mesh transparency (left) and corresponding radiation spectra (right) (the results are given for resonator #3, refer to [7] for all dimensions details).

For configuration *2* and *3*, however, at $z = 0$, one more maximum of the oscillating current component is observed. This confirms the presence of two main periodic processes in the vircator, associated with oscillations of the VC itself and with oscillations of electrons in the potential well "cathode – VC". All our numerous calculations, however, show that the frequencies of these oscillations are always the same, and they are determined primarily by the frequency of electron oscillations between the real and virtual cathodes. This means that in real vircators, there is a single self-consistent generation mechanism: the oscillations of electrons and VCs are strongly coupled (they aren't independent). What has been said, in our opinion, is qualitatively very well illustrated, for example, in the paper [4] (p. 950). Unfortunately, at present, researchers often overlook this circumstance and talk about two different *independent* generation mechanisms in vircators.

High current beams are used for the practical realization of high-power vircators; the anode is typically constructed from a metal mesh with some finite value of transparency for electrons. The cathode-anode gap is diminished during the pulse, and anode mesh transparency can also change due to plasma expanding effects. To clarify the effect of the transparency, we carried out a series of simulations with a resonant vircator (configuration *3*). Fig. 6 shows the calculated dependence of the generation power on the transparency of the anode mesh. For each value of the cathode-anode gap, there is a well-defined optimal value of mesh transparency at which the radiation power has a maximum. If transparency is higher than optimal, power and efficiency drop sharply because the plasma frequency of the beam behind the mesh becomes too high, and, as a result, the generation frequency is far from the resonator's natural frequency. In essence, the generation efficiency in this case is the same as that of a non-resonant vircator. Changing the transparency to be below the optimal value leads to a decrease in the beam current (power) passing through the mesh, so the efficiency also gradually decreases, dropping to zero when the current becomes insufficient for the formation of VC.

4. Conclusion

The presented work is devoted to numerical simulation of the generation processes in an axial vircator. The generation phenomena have been analyzed in two scenarios: with and without considering cathode-anode gap processes. A comparative analysis between the two principal layouts, injection of the high-current electron beam into a simple drift tube and into the resonator, is also presented. The main results of the presented work can be summarized as follows:

1. The generation mechanisms in vircators with and without considering the cathode-anode gap phenomena are significantly different; even the generation frequencies differ radically.
2. When taking into account the phenomena in the gap (which is required for most practical problems), regardless of the transparency of the anode mesh, a mode is realized in which the oscillations of electrons between the real and virtual VC and the oscillations of the VC itself occur synchronously (consistently), always with the same frequency. This frequency is inversely proportional to the value of the cathode-anode gap and can be described well by the formula (3).
3. Effective generation in a resonant vircator is possible when the resonator's natural frequency is close enough to the radiation frequency of the vircator without a resonator.
4. The dependencies of generation efficiency on the beam current, cathode-anode gap value, and anode mesh transparency were calculated. The most important and principal conclusion concerning the vircator generation nature is that for each geometry of the resonator, there is an optimal value of anode mesh transparency, maximizing the generation efficiency and power.

5. References

[1] W. Jiang, M. Kristiansen, Theory of virtual cathode oscillator, *Phys. Plasmas*, vol. **8**(8), 3781, 2001; doi: 10.1063/1.1382643

[2] A.N. Didenko, The mechanism of the powerful microwave oscillations generation in vircator, *Doklady Akademii Nauk SSSR [in Russian] (Proc. of the USSR Academy of Sciences)*, vol. **321**(4), 727, 1991.

[3] A.A. Rukhadze, S.D. Stolbetsov, V.P. Tarakanov, Vircators, *Radiotekhnika i elektronika [in Russian]*, vol. **37**(3), 385, 1992.

[4] B.V. Alyokhin, A.E. Dubinov, V.D. Selemir [et al.], Theoretical and experimental studies of virtual cathode microwave devices, *IEEE Trans. Plasma Sci.*, vol. **22**(5), 945, 1994; doi: 10.1109/27.338312

[5] A.N. Didenko, V.I. Rashchikov, High power microwave generation in virtual cathode systems, *1991 IEEE Particle Accelerator Conference*, San Francisco, USA, 3111, 1991; doi: 10.1109/PAC.1991.165204

[6] J.P. Verboncoeur, A.B. Langdon, N.T. Gladd, An Object-Oriented Electromagnetic PIC Code, *Comp. Phys. Comm.*, vol. **87**, 199, 1995; doi: 10.1016/0010-4655(94)00173-Y

[7] E.A. Gurnevich, P.V. Molchanov, The effect of the electron-beam parameter spread on microwave generation in a three-cavity axial vircator, *IEEE Trans. Plasma Sci.*, vol. **43**(4), 1014, 2015; doi: 10.1109/TPS.2015.2407492

[8] W. Woo, Two-dimensional features of virtual cathode and microwave emission, *The Physics of fluids*, vol. **30**(1), 239, 1987; doi: 10.1063/1.866181